Cone Penetration Testing 2022 – Gottardi & Tonni (eds)

Kriging analysis on CPTU data from offshore wind farm

Rongjie He & Jinhui Li*
Department of Civil and Environmental Engineering, Harbin Institute of Technology (Shenzhen), China

Shaoli Yang
Norwegian Geotechnical Institute (NGI), Oslo, Norway

Ben He
Key Laboratory for Far-shore Wind Power Technology of Zhejiang Province; PowerChina Huadong Engineering Corporation Limited, (HDEC), Hangzhou, China

ABSTRACT: In recent years, offshore wind power has been widely developed. Because of the complexity of marine geology and the large spatial variability of soils, it is necessary to obtain CPTU data before the foundation design. However, how to reasonably interpret the CPTU data will greatly affect the reliability and safety of the offshore windfarm foundation. In addition, there is a need to predict soil conditions at the locations without CPTU data. In this study, based on the available CPTU data of offshore wind farm in east China sea, kriging method is used to interpret the CPTU data, and the soil conditions in a large area can be predicted. This method can be used to develop ground model for a large offshore wind farm, and estimate the relevant soil parameters based on CPTU data. The analysis methods can provide reference for other projects of offshore wind farm.

Keywords: offshore wind farm, CPTU, kriging method, marine geology

1 INTRODUCTION

Offshore wind power has been widely used as the clean energy in many countries. Dinh and Nguyen (2019) proposed that offshore wind power has the advantages of higher full load hours per year, longer service life and higher rotor speed comparing with onshore wind power. In practical engineering, foundation design should be carried out before the installation of offshore wind turbine.

Marine soil has the characteristics of large spatial variability (Dasaka and Zhang 2012; Ching and Phoon 2013; Li et al. 2014; Lloret-Cabot et al. 2014). Before the foundation design of the offshore wind turbine, it is necessary to obtain the CPTU data of relevant soil layers. Then the obtained CPTU data can be interpreted to get soil parameters. For example, Robertson method (Robertson and Wride, 1998) can be used to determine the classification of marine soil layer based on the CPTU data. However, due to the high cost of offshore work, the CPTU tests in a large area are usually limited. Therefore, how to predict soil conditions at the locations without CPTU data has become an important engineering problem which needs to be solved.

Based on the above background, taking the CPTU data of offshore wind farm in east China sea as an example, this study used the Kriging method to predict the CPTU data in the unknown area, and then used the Robertson method (Robertson and Wride, 1998) to obtain the soil classification of the whole seabed profile. The predicted results can reach the 95% confidence interval in statistics. The algorithm can provide reference and guidance for the foundation design of offshore wind turbine.

2 INVESTIGATION SITE OF OFFSHORE WIND FARM

The site of the offshore wind farm is in the east China sea. The positions of the boreholes are shown in Figure 1. This site contains 27 boreholes. The drilling depth of each borehole is more than 35 m, and CPTU data is measured every 0.02 m along the

*Corresponding author
DOI: 10.1201/9781003308829-144

depth. In Figure 1, the interval of boreholes in different columns is 11000 m which is too large, so 15 boreholes in the same column are selected for analysis as shown in the frame. The measured CPTU data contain cone penetration resistance (q), sleeve friction (f) and pore pressure (u).

According to the soil samples at the site, the actual soil layers of boreholes no. 50, no. 72 and no. 77 have been already known which are shown in Figure 2. It can be seen from Figure 2 that the actual seabed geological conditions are generally divided into four layers: Ooze clay, clay, silty clay, and silty sands. The soil layers in the first 25 m are relatively homogeneous, and they are Ooze clay. The soil layers beyond 25 m vary from location to location. Figure 3 shows the typical CPTU data along depth of borehole no. 50. It can be seen that the trend of the curve at the first 25 m is increasing linearly, and the trend of the curve is much more complicated beyond 25 m.

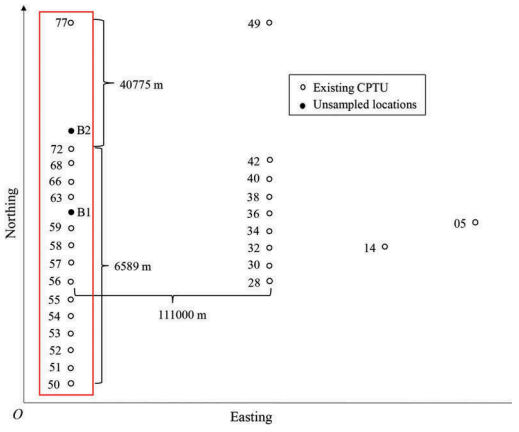

Figure 1. The position of the boreholes.

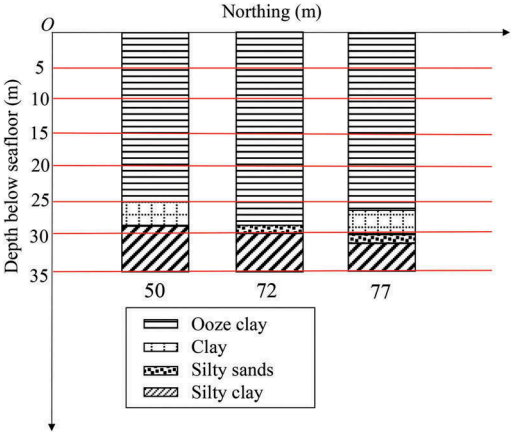

Figure 2. Soil conditions of known boreholes (Borehole no. 50, no. 72 and no. 77).

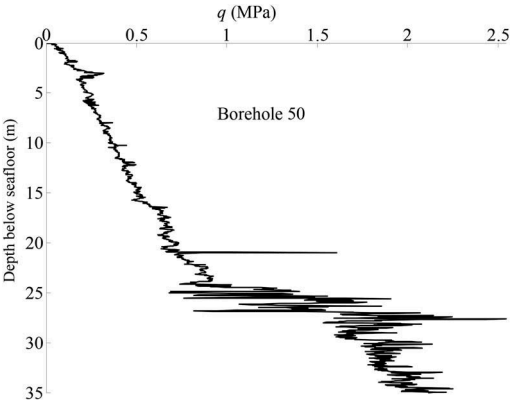

Figure 3(a). Measured cone resistance along depth below seafloor

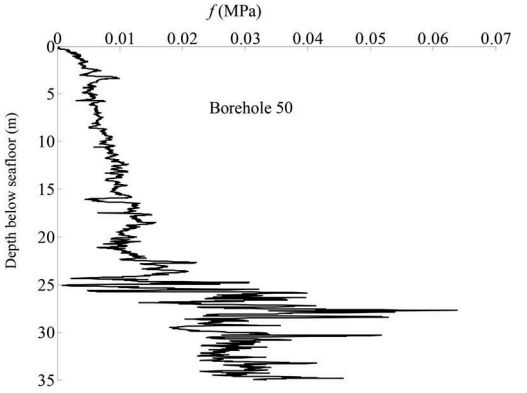

Figure 3(b). Measured sleeve friction along depth below seafloor

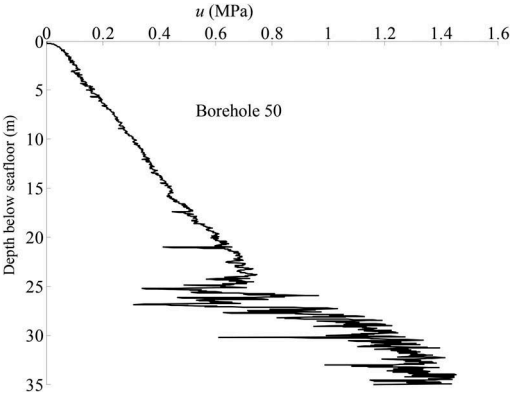

Figure 3(c). Measured pore pressure along depth below seafloor.

Figure 3. The variation of CPTU data with depth in borehole no. 50.

Based on CPTU data, the classification of soil layer can be obtained. There are many traditional

soil classification methods, such as Jefferies method (Jefferies and Davies, 1991), Olsen method (Olsen and Mitchell, 1995), Robertson method (Robertson and Wride, 1998) and so on. Liu et al. (2013) proposed that the Robertson method is suitable for the Chinese soil classification. Therefore, the Robertson method is used for soil classification in this study. The calculation formulas are shown from Equation 1 to Equation 6,

$$Q_{\mathrm{tn}} = \frac{q_{\mathrm{t}} - \sigma_{\mathrm{v0}}}{\sigma'_{\mathrm{v0}}} \tag{1}$$

$$F_{\mathrm{r}} = \frac{f_{\mathrm{s}}}{q_{\mathrm{t}} - \sigma_{\mathrm{v0}}} \times 100\% \tag{2}$$

$$B_{\mathrm{q}} = \frac{u - u_0}{q_{\mathrm{t}} - \sigma'_{\mathrm{v0}}} \tag{3}$$

$$I_{\mathrm{c}} = \sqrt{[3.47 - \lg\,(Q_{\mathrm{tn}})]^2 + [\lg\,(F_{\mathrm{r}}) + 1.22]^2} \tag{4}$$

$$q_t = q + (1 - a)u \tag{5}$$

$$a = d^2/D^2 \tag{6}$$

where Q_{tn} is normalized cone penetration resistance; F_r is normalized sleeve friction; B_q is normalized pore pressure; σ_{v0} is the total overburden stress; σ'_{v0} is effective overburden stress; u_0 is equilibrium pore pressure; q_{t} is corrected cone penetration resistance; a is the net area ratio between load cell support diameter, d, and cone diameter, D; I_c is soil classification index. The soil types are attributed from I_{c} which is shown in Table 1.

Table 1. The soil classification based on Robertson method.

I_c	Soil type
I_c>3.6	Ooze clay
2.95<I_c<3.6	Clay
2.60<I_c<2.95	Silty clay
2.05<I_c<2.60	Sandy silt
1.31<I_c<2.05	Silty sands
I_c<1.31	Dense sand

3 KRIGING METHOD

Kriging interpolation (Liu et al., 2016) is an optimal linear unbiased interpolation method. For ordinary Kriging, there is a group of observation points in region D, whose position coordinates are x_1, x_2, x_3 to x_{n}, respectively, and the corresponding observation values are $Z(x_1)$, $Z(x_2)$, $Z(x_3)$ to $Z(x_{\mathrm{n}})$, respectively. Then the formula of the estimated value at unknown position x_0 in region D is shown in Equation 7,

$$Z^*(x_0) = \sum_{i=1}^{n} \lambda_i Z(x_i) \tag{7}$$

where λ_i is the weight coefficient of Kriging interpolation. The values of λ_i should be known. The semivariogram is used to calculate the λ_i. The semivariogram of the observation data can be calculated by Equation 8,

$$\gamma(h) = \frac{1}{2N_h} \sum_{i=1}^{N_h} [Z(x_i + h) - Z(x_i)]^2 \tag{8}$$

where N_h is the number of the observation points and h is the separation distance between different points. Based on the semivariogram values of the observation points, the Gaussian model and exponential model are usually used to fit the trend of the semivariogram which are shown in Equation 9 and Equation 10,

$$\gamma(h) = C_0 + C(1 - e^{-\frac{3h^2}{a^2}}) \tag{9}$$

$$\gamma(h) = C_0 + C(1 - e^{-\frac{3h}{a}}) \tag{10}$$

where C_0 is nugget; C is partial sill and a is range. Before fitting the semivariogram, it is essential that the data is stationary; that is, the mean and covariance of the data depend only upon separation, not on absolute location. If the data are non-stationary, treatment must be given to transform the data to a stationary set by removing the deterministic component called the trend, and the stationary residual random component is then analyzed.

After fitting the semivariogram, the weight coefficient λ_i can be calculated based on Equation 11,

$$\begin{bmatrix} \gamma_{11} & \gamma_{12} & \cdots & \gamma_{1n} & 1 \\ \gamma_{21} & \gamma_{22} & \cdots & \gamma_{2n} & 1 \\ \vdots & \vdots & & \vdots & 1 \\ \gamma_{n1} & \gamma_{n2} & \cdots & \gamma_{nn} & 1 \\ 1 & 1 & \cdots & 1 & 0 \end{bmatrix} * \begin{bmatrix} \lambda_1 \\ \lambda_2 \\ \vdots \\ \lambda_n \\ \mu \end{bmatrix} = \begin{bmatrix} \gamma_{01} \\ \gamma_{02} \\ \vdots \\ \gamma_{0n} \\ 1 \end{bmatrix} \tag{11}$$

where γ_{ij} is the modelled semivariogram values based on the distance between the two samples pertaining to

the ith and jth locations, and μ is the Lagrange parameter. The formula for calculating the variance is shown in Equation 12,

$$\sigma_{OK}^2 = \sum_{i=1}^{n} \lambda_i \gamma_{0i} + \mu \tag{12}$$

where σ_{OK} is the OK standard variance of the Kriging method. Assuming that the parameter is normally distributed with a mean value z_0 (estimated value) and a standard variance σ_{OK}, the 95% confidence interval of the estimation is [z_0-1.96σ_{OK}, z_0+1.96σ_{OK}] (Ang and Tang, 2007).

Taking the CPTU data in depth 10 m for analysis as an example, the fitting equations of the deterministic component are shown in Equation 13, Equation14 and Equation 15, respectively,

$$q_{trend} = 0.2871x - 34.2453 \tag{13}$$

$$f_{trend} = 0.0061x - 0.7291 \tag{14}$$

$$u_{trend} = 0.5127x - 61.5089 \tag{15}$$

where q_{trend}, f_{trend} and u_{trend} are trend values of cone penetration resistance, sleeve friction and pore pressure, and x is the longitude coordinate of the observation points.

After removing the deterministic component, the stationary residual random components are used to fit the semivariogram. In this case study, comparing with Gaussian model, exponential model has higher fitting goodness. As a result, the exponential function is used to fit the semivariogram. The number of lag distances is 105 in total. Taking about 200 m as a group, the lag distances are divided into 14 groups. The lag distances of 14 groups are averaged to obtain the best fitting results and they are shown in Figure 4.

Cheon and Gilbert (2014) indicated that it is reasonable to have a horizontal range of more than 1000 m in offshore engineering. Based on the results, the range of the three residuals are all 120 m which are reasonable. Then, the CPTU data in unknown positions can be predicted based on the modelled semivariogram.

4 PREDICTION OF SOIL TYPES

From Figure 2, there are mainly four soil layers in the seabed. According to the calculation, different soil layers have different modelled semivariograms. As a result, four modelled semivariograms were used to analyze the depths below seafloor at depth of 1m to 25 m, 26 m to 29 m, 29 m to 31 m, and 31 m to 35 m, respectively.

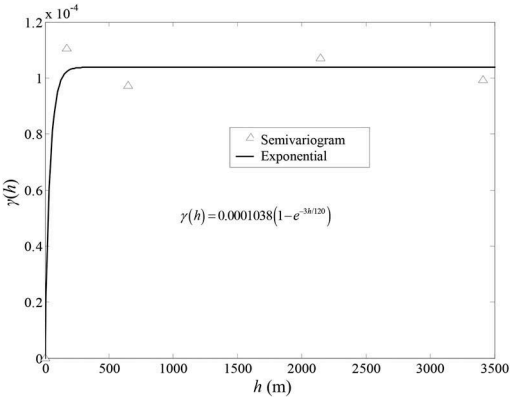

Figure 4(a). The semivariogram of cone resistance

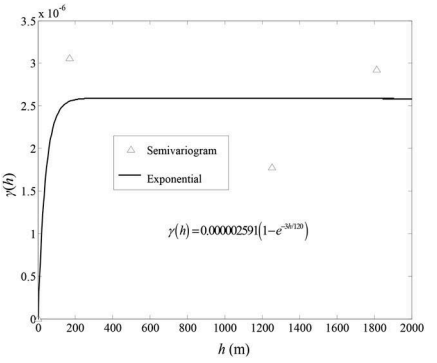

Figure 4(b). The semivariogram of sleeve friction

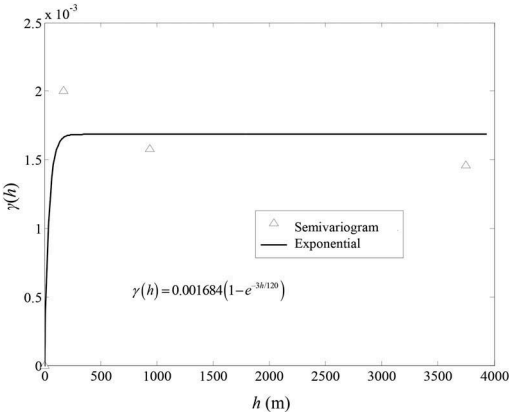

Figure 4(c). The semivariogram of pore pressure

Figure 4. The semivariogram of CPTU data in depth 10 m.

In order to verify the accuracy of the Kriging method, the soil types at boreholes no. 50 and no. 77 were predicted. The predicted results are shown in

Figure 5 and Figure 6. The results were compared with the actual soil types at the two boreholes. It can be seen that the predicted soil types are basically consistent with the actual soil types. The results prove that the Kriging method is reasonable.

B1 is the first unknown position without CPTU data which needs to be predicted. The longitude and latitude of B1 are 120.556 degree and 27.14 degree, respectively. For the depth of 15 m, 27 m, 30 m and 35 m, the estimators of cone penetration resistance of B1 are 0.521 MPa, 1.213 MPa, 2.105 MPa and 3.290 MPa; the estimators of sleeve friction of B1 are 6.7 kPa, 18 kPa, 21.3 kPa and 61.3 kPa, and the estimators of pore pressure of B1 are 0.414 MPa, 0.601 MPa, 0.808 MPa and 0.822 MPa. The 95% interval of confidence is shown in Table 2 and the predicted soil types are shown in Figure 7. For Table 2, it just means that the value will be within this interval.

Table 2. The predicted CPTU data in B1 (95% confidence interval).

Depth (m)	q (MPa)	f (kPa)	u (MPa)
15	[0.521, 0.521]	[6.690, 6.705]	[0.411, 0.418]
27	[1.106, 1.321]	[17.3, 18.7]	[0.572, 0.630]
30	[0, 8.794]	[20.80, 21.8]	[0.443, 1.173]
35	[0, 31.725]	[0.056, 0.067]	[0.176, 1.469]

B2 is the second unknown position without CPTU data which also needs to be predicted. The longitude and latitude of B2 are 120.592 degree and 27.14 degree, respectively. For the depth of 15 m, 27 m, 30 m and 35 m, the estimators of cone penetration resistance of B2 are 0.520 MPa, 1.186 MPa, 2.038 MPa and 3.066 MPa; the estimators of sleeve friction of B2 are 6.8 kPa, 17.3 kPa, 21.5 kPa and 57.3 kPa, and the estimators of pore pressure of B2 are 0.414 MPa, 0.643 MPa, 0.760 MPa and 0.827 MPa. The 95% interval of confidence is shown in Table 3. For Table 3, it just means that the value will be within this interval.

According to the soil classification criteria, the predicted soil types are the same with that at location B1, which can be seen in Figure 7.

Table 3. The prediction CPTU data in B2 (95% confidence interval).

Depth (m)	q (MPa)	f (kPa)	u (MPa)
15	[0.52, 0.52]	[6.79, 6.805]	[0.410, 0.417]
27	[1.081, 1.291]	[16.6, 18.02]	[0.622, 0.665]
30	[0, 8.636]	[0.021,0.022]	[0.415, 1.104]
35	[0, 30.797]	[0.052, 0.062]	[0.189, 1.465]

Based on the CPTU data of boreholes, the seabed profile can be predicted and the results are shown in

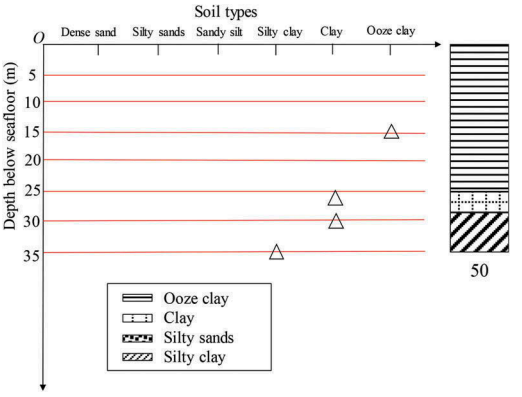

Figure 5. The comparison between prediction value and actual data in borehole no. 50.

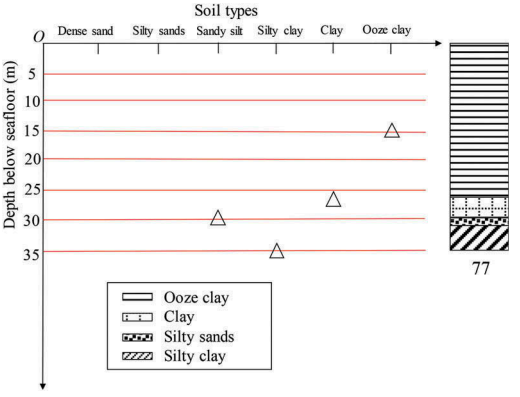

Figure 6. The comparison between prediction value and actual data in borehole no. 77.

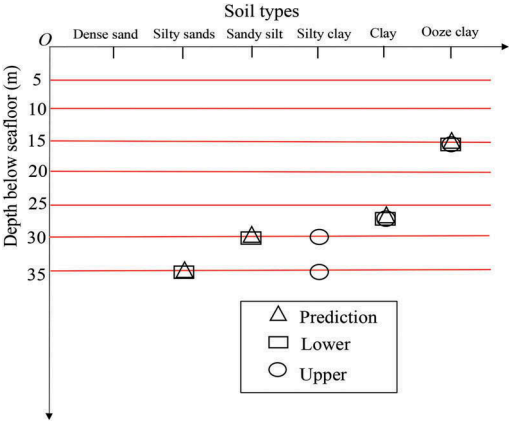

Figure 7. The prediction of soil classification in B1 and B2 (95% CI).

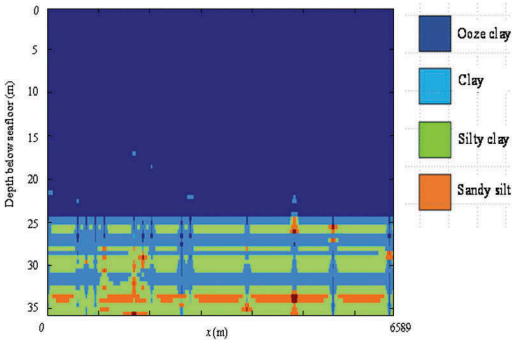

Figure 8. The prediction soil layer of seabed profile.

Figure 8. It can be seen that the seabed profile mainly has four soil layers containing ooze clay, clay, silty clay and sandy silt. In the first 25 m, the soil is homogeneous which is ooze clay. Beyond 25 m, the soil conditions become much more complex. The general conditions of soil layer are consistent with the actual soil conditions. It means that Kriging method can predict the soil conditions at unknown positions effectively, which can be used to guide the foundation design of offshore wind turbine.

5 CONCLUSIONS

In this study, the offshore wind farm in east China sea is analyzed as a case study. The results indicate that Robertson method is suitable for the soil classification in the east China sea and Kriging method can predict the soil conditions in unknown positions with 95% interval of confidence. The algorithm can be used to provide guidance and reference for the foundation design of offshore wind turbine.

ACKNOWLEDGMENTS

This study is supported by Key Laboratory for Farshore Wind Power Technology of Zhejiang Province and Norwegian Geotechnical Institute (NGI). This work was supported by the Natural Science Foundation of China [grant number 51979067] and Shenzhen Technology Innovation Project [grant number JCYJ20210324121402008].

REFERENCES

Ang, A.H.S. & W.H. Tang (2007). Thin layer effects on the CPT q_c measurement. Canadian Geotechnical Journal, 42 (5), 1302–1307.

Ching, J. & K.K. Phoon (2013). Probability distribution for mobilized shear strengths of spatially variable soils under uniform stress states. Georisk, 7 (3), 209–224.

Cheon, J.Y & R.B. Gilbert (2014). Modeling spatial variability in offshore geotechnical properties for reliability-based foundation design. Structural Safety. 49 (2014), 18–26.

Dasaka, S.M. & L.M. Zhang (2012). Spatial variability of in situ weathered soil. Geotechnique, 62 (5), 375–384.

Dinh, V.N. & H.X. Nguyen (2019). Design of an offshore wind farm layout. Lecture Notes in Civil Engineering, 2019, 18, 233–238.

Jefferies, M.G. & M.P. Davies (1991). Soil classification by the cone penetration test: Discussion[J]. Canadian Geotechnical Journal, 28 (1), 173–176.

Li, J.H., Huang, J., Cassidy, M.J., & R. Kelly (2014). Spatial variability of the soil at the Ballina National Field Test Facility. Australia Geomechanics, 49 (4), 41–47.

Li, J.H., Cassidy, M.J., Huang, J., Zhang, L., & R. Kelly (2016). Probabilistic identification of soil stratification. Geotechnique, 66 (1), 16–26.

Liu, S.Y., Cai, G.J., & H.F. Zhou (2013). Practical soil classification methods in China based on piezocone penetration tests. Journal of Geotechnical Engineering, 35 (10), 1765–1775 [in Chinese].

Lloret-Cabot, M., Fenton, G.A., & M.A Hicks (2014). On the estimation of scale of fluctuation in geo-statistics. Georisk, 8 (2), 129–140.

Olsen, R.S. & J.K. Mitchell (1995). CPT stress normalization and prediction of soil classification. Proceedings of International Symposium on Cone Penetration Testing, CPT'95, Linköping, Sweden, SGI Report 3:95, 2, 257–262.

Robertson P.K. & C.E. Wride (1998). Evaluating cyclic liquefaction potential using the cone penetration test. Canadian Geotechnical Journal, 35 (3), 442–459.